Antiproliferative Effect of Elastin-Derived Peptide VGVAPG on SH-SY5Y Neuroblastoma Cells

Konrad A. Szychowski[1] · Agnieszka Rombel-Bryzek[1] · Agnieszka Dołhańczuk-Śródka[2] · Jan Gmiński[3]

Abstract

Throughout the lifetime of humans, the amount of stem cells and the rate of cell proliferation continue to decrease. Reactive oxygen species (ROS) are one among the many factors that promote stem cell aging. Both a decrease in the level of stem cells and increase in ROS production can lead to the development of different neurodegenerative diseases. This study was conducted to determine how the VGVAPG peptide, liberated from elastin during the aging process and under pathological conditions, affects ROS production and activities of antioxidant enzymes in undifferentiated, proliferating SH-SY5Y cells. SH-SY5Y cells were maintained in Dulbecco's modified Eagle's medium/nutrient mixture F-12 supplemented with 10% heat-inactivated fetal bovine serum (FBS). After treating the SH-SY5Y cells with VGVAPG peptide, we measured ROS production; cell metabolism, proliferation, and expression; and activities of superoxide dismutase (SOD), glutathione peroxidase (GPx), and catalase (CAT). We demonstrated that the VGVAPG peptide increases GPx expression and activity, whereas it decreases CAT expression in SH-SY5Y cells. Silencing of the *GLB1* gene prevents changes in GPx activity. Despite the fact that the VGVAPG peptide increases GPx expression, it increases the ROS level. Moreover, the VGVAPG peptide decreases SH-SY5Y proliferation, which is prevented by the ROS scavenger *N*-acetyl-L-cysteine. Our data suggest that ROS production and decreased proliferation of SH-SY5Y cells are the results of excitotoxicity meditated through close unrecognized molecular pathways. More research is needed to elucidate the unknown mechanism of action of VGVAPG peptide in the nervous system.

Highlights

- VGVAPG peptide increases ROS production in SH-SY5Y cells
- VGVAPG increases GPx expression and activity in SH-SY5Y cells
- VGVAPG decreases expression of CAT enzymes in SH-SY5Y cells
- VGVAPG decreases SH-SY5Y proliferation
- Silencing of *GLB1* gene prevents VGVAPG-induced increase in GPx activity
- VGVAPG affects PPARγ expression in the SH-SY5Y cell line

✉ Konrad A. Szychowski
konrad.szychowski@gmail.com

[1] Department of Clinical Biochemistry and Laboratory Diagnostics, Institute of Medicine, University of Opole, Oleska 48, 45-052 Opole, Poland

[2] Institute of Biotechnology, University of Opole, Kard. B. Kominka 6a, 45-032 Opole, Poland

[3] Department of Public Health, Dietetics and Lifestyle Disorders, Faculty of Medicine, University of Information Technology and Management in Rzeszow, Sucharskiego 2, 35-225 Rzeszow, Poland

Introduction

Throughout the human lifetime, the amount of stem cells and rate of cell proliferation continue to decrease (Apple et al. 2017). The presence of reactive oxygen species (ROS) is one among the many factors that promote stem cell aging (Oh et al. 2014). To date, it has been described that the decrease in stem cell level and increase in ROS production can both lead to the development of different neurodegenerative diseases (Kim et al. 2015). During the aging process and with exposure to xenobiotics, there is a consequent increase in ROS levels in the brain that then generates a snowball phenomenon (Kołodziej et al. 2018). Moreover, ROS have been suggested to be involved in the evolution of cellular damage caused by ischemia–reperfusion, anoxia–reperfusion, and hypoxia–reperfusion (Sasaki et al. 2018). ROS damages the cells and walls of brain capillaries, and this leads to the release of elastin-derived peptides (EDPs) from the extracellular matrix (ECM) (Nita and Grzybowski 2016). In the elastin molecule,

the VGVAPG peptide is the most important sequence—one that is repeated many times and is easily liberated from either elastin or EDPs under physiological and pathological conditions (Senior et al. 1984; Gminski et al. 1993). It is well documented that the VGVAPG sequence (alone or as a part of EDPs) binds with high affinity to elastin-binding protein (EBP) located on the cell surface (Senior et al. 1984; Blood et al. 1988). EBP is a catalytically inactive form of the alternatively spliced gene for β-galactosidase (*GLB1* gene) (Hinek et al. 1993; Skeie et al. 2012). The second receptor for the VGVAPG peptide is galectin-3, which also has an important role in cell–ECM interactions (Ochieng et al. 2002). Galectin-3 is mostly expressed in inflammatory cells (Bresalier et al. 1996; Cantarelli et al. 2009); however, its expression has been linked with tumor progression, cancer aggressiveness, and melanoma invasiveness (Ochieng et al. 1999; Pocza et al. 2008; Wang et al. 2009).

Studies, to date, have reported that EDPs induce ROS production in monocytes and human fibroblasts (Robert et al. 1984; Scandolera et al. 2015). Our previous research showed that ROS levels increase during stimulation with VGVAPG peptide in mouse primary astrocytes in vitro (Szychowski and Gmiński 2019a). It has been described that EDPs enhance the activities of antioxidant enzymes, such as superoxide dismutase (SOD), catalase (CAT), or glutathione peroxidase (GPx), and increase lipid peroxidation in human fibroblasts (Gmiński et al. 1991). Moreover, the VGVAPG peptide reduced ROS production in neutrophils in control patients and those with stable chronic obstructive pulmonary disease (COPD) (Dupont et al. 2013). Interestingly, at low concentrations, ROS can act as signaling molecules in both intra- and extracellular signal transduction pathways to influence a variety of cellular processes, such as proliferation, metabolism, differentiation, and survival (Glennon-Alty et al. 2018).

The involvement of the VGVAPG peptide and EDPs in cell proliferation is well documented in human skin fibroblasts, in the cytotrophoblast in first-trimester placental explants, in astrocytoma and glioblastoma cell lines, as well as in porcine coronary arterial smooth muscle cells (Kamoun et al. 1995; Jung et al. 1998; Mochizuki et al. 2002; Coquerel et al. 2009; Desforges et al. 2014). Cell proliferation is mainly associated with the activation of EBP and, less often, with galectin-3, which is mainly involved in cell migration (Inohara et al. 1998; Toupance et al. 2012).

Human neuroblastoma (SH-SY5Y) cells maintain their potential for proliferation and differentiation under culture conditions and display some properties of stem cells (Walton et al. 2004; Hämmerle et al. 2013; Ross et al. 2015). Therefore, because of their stemness, SH-SY5Y cells can be used as a model of undifferentiated neuroblasts to test cell proliferation (Walton et al. 2004; Hämmerle et al. 2013). Recent data have shown that SH-SY5Y cells are a good model for testing ROS-dependent apoptosis and cell proliferation in neurological conditions such as Alzheimer's and Parkinson's disease (Uğuz et al. 2016; Venkatesh Gobi et al. 2018). Moreover, an increase in ROS production in the SH-SY5Y cell line can be associated with autophagy, which is present in neurological diseases (Chiappini et al. 2018).

This study was conducted with an aim to determine how the VGVAPG peptide affects ROS production as well as the expression and activities of antioxidant enzymes in undifferentiated, proliferating SH-SY5Y cells.

Materials and Methods

Reagents

DMEM/F12 1:1 (16–405-CVR) without phenol red was purchased from Corning (Manassas, VA, USA). Trypsin, streptomycin, penicillin, glycerol, CHAPS, HEPES, dithiothreitol (DTT), NaCl, EDTA, dimethyl sulfoxide (DMSO), 2′,7′-dichlorodihydrofluorescein diacetate (H_2DCFDA), and *N*-acetyl-L-cysteine (NAC) were purchased from Sigma-Aldrich (St. Louis, MO, USA). The FastStart Universal Probe Master (Rox) was purchased from Roche Applied Science (Mannheim, Germany). The *GLB1* siRNA (sc-43792) and *LGALS3* (sc-155994) were purchased from Santa Cruz Biotechnology (Santa Cruz, CA, USA). The VGVAPG and VVGPGA peptides were synthesized by LipoPharm.pl (Gdańsk, Poland). Heat-inactivated fetal bovine serum (FBS) was purchased from EURx (Gdańsk, Poland). The High-Capacity cDNA Reverse Transcription Kit and the TaqMan® probes corresponding to specific genes encoding *ACTB* (Hs01060665_g1), *PPARγ* (Hs00234592_m1), and *KI67* (Hs04260396_g1) were obtained from Life Technologies Applied Biosystems (Foster City, CA, USA). Peroxisome proliferator-activated receptor gamma (PPARγ; E-EL-H1361), SOD1 (E-EL-H1113), and GPx (E-EL-H5410) ELISA assays as well as CAT (E-BC-K031), SOD (E-BC-K020), and GPx (E-BC-K096) activity assays were obtained from Elabscience Biotechnology (Wuhan, China). CAT (EH0643) and Ki67 (EH0684) ELISA assays were obtained from Wuhan Fine Biotech Co., Ltd. (Wuhan, China). Stock solutions of the VGVAPG and VVGPGA peptides were prepared in DMSO and added to the DMEM/F12 medium. The final concentration of DMSO in the culture medium was always 0.1%.

SH-SY5Y Cell Culture

The human neuroblastoma (SH-SY5Y) cell line were obtained from the American Type Culture Collection (ATCC distributor: LGC Standards, Łomianki, Poland). SH-SY5Y cells were maintained in DMEM/F12 medium supplemented with 10% heat-inactivated FBS at 37 °C in a

humidified atmosphere with 5% CO_2. The cells were seeded in 96-well culture plates at a density of 6×10^3 (for 6- and 24-h treatment) and 5×10^3 (for 48-h treatment) per well, and initially cultured for 24 h prior to the experiment. Subsequently, the medium was changed to a fresh medium by increasing the concentrations (100 pM; 1, 10, 50, and 100 nM; and 1, 10, 50, and 100 μM) of the VGVAPG peptide.

siRNA Gene Silencing Procedure

GLB1 and *LGALS3* siRNA were used to inhibit the expression of EBP and galectin-3 in the SH-SY5Y cell line. The experiment was conducted in accordance with a previously described procedure (Szychowski et al. 2019a). Briefly, *GLB1* and *LGALS3* siRNA were applied for 7 h at a final concentration of 50 nM in an antibiotic-free medium containing the siRNA transfection reagent INTERFERin. After transfection, the culture medium was changed to normal culture medium and the SH-SY5Y cells were cultured for 12 h prior to commencing the experiment. Vehicle controls included positive siRNA and scramble siRNA containing a scrambled sequence that did not lead to specific degradation of any known cellular mRNA.

Measurement of ROS Production

The ROS measurement was undertaken according to a previously described method (Szychowski and Wójtowicz 2016). To determine the ability of the VGVAPG peptide to induce ROS production in the selected cells, 5 μM H_2DCFDA was applied. The cells were then incubated in H_2DCFDA in serum-free and phenol red–free medium for 45 min prior to treatment with compounds. After 3-, 6-, and 24-h incubation of the cells with increasing concentrations of compounds (5% CO_2 at 37 °C), the culture medium was replaced with fresh medium to remove the extracellular residual DCF and the studied compound to reduce the background fluorescence. Cells treated with 0.3% hydrogen peroxide (H_2O_2) were used as a positive control (result not shown). DCF fluorescence was measured using a microplate reader (FilterMax F5) at maximum excitation and emission spectra of 485 and 535 nm, respectively.

Resazurin Reduction Assay

The resazurin reduction cell viability and metabolism assay was conducted according to a previously described method (Szychowski et al. 2017a). On the day of analysis, a working solution of 60 μM resazurin was prepared in a medium containing 1% FBS. After 24- and 48-h treatment, cells with increasing concentrations of the VGVAPG peptide medium in the wells were replaced into a working solution of resazurin (100 μL) and the plates were placed in 37 °C. Fluorescence

was measured with excitation and emission wavelengths of 530 and 590 nm, respectively, on a FilterMax F5 Multi-Mode microplate reader (Molecular Devices, Corp., Sunnyvale, CA, USA) for 30 min and 1 h after dye addition.

Real-Time PCR Analysis of mRNAs Specific to Genes Encoding *Ki67* and *PPARγ*

For the real-time PCR assay, the SH-SY5Y cell line was seeded on six-well plates and initially cultured for 24 h. After 6-h exposure to 50 nM and 1 μM of VGVAPG, samples of total RNA were extracted from the SH-SY5Y cell line in accordance with the manufacturer's protocol, based on a previously described method (Szychowski et al. 2017b). After siRNA transfection, the procedure was undertaken after exposure to a concentration of 50 nM and 1 μM VGVAPG for 6 h. The RNA quality and quantity were determined spectrophotometrically at 260 and 280 nm, respectively (ND/1000 UV/Vis; Thermo Fisher NanoDrop, USA). Two-step quantitative real-time reverse transcription (qRT) PCR was conducted using the CFX Real-Time System (BioRad, USA). The RT reaction was carried out at a final volume of 20 μL with 180 ng of RNA (as a cDNA template) by using the cDNA reverse transcription kit according to the manufacturer's instructions. Briefly, the reaction was conducted for 10 min at 25 °C, then 120 min at 37 °C, next for 5 min at 85 °C, and thereafter held at 4 °C. Between analyses, cDNA was stored at − 80 °C. Products from the RT reaction were amplified using the FastStart Universal Probe Master (Rox) kit with TaqMan probes as primers for specific genes encoding *ACTB*, *PPARγ*, and *KI67* according to the manufacturer's protocol. Amplification was carried out in a total reaction volume of 20 μL containing 1.0 μL RT product; *ACTB* was used as the reference gene. A standard qPCR procedure was utilized: the reaction was conducted for 2 min at 50 °C and 10 min at 95 °C, followed by 40 cycles of 15 s at 95 °C and 1 min at 60 °C. Random peptide sequence VVGPGA was used as a control, and did not affect *PPARγ* and *KI67* mRNA expression (data not shown). The threshold value (Ct) for each sample was set during the exponential phase, and the ΔCt method was used for data analysis. To study the gene expression levels, three candidate reference genes (*Actb*, *Gapdh*, and *18S*) were selected and validated. To evaluate the reference gene expression, we used the RefFinder web-based comprehensive tool, which integrates major computational programs (geNorm, Normfinder, BestKeeper, and the comparative ΔCt method) for comparison and ranking of candidate reference genes.

ELISA for Ki67, PPARγ, SOD1, CAT, and GPx

Levels of Ki67, PPARγ, SOD1, CAT, and GPx proteins were determined via ELISA after 24- and 48-h treatment with

50 nM and 1 μM VGVAPG. Specific detections of these proteins were obtained using ELISA and they were subsequently subjected to quantitative sandwich enzyme immunoassay. The assay was conducted according to the manufacturer's instructions from Elabscience Biotechnology and Wuhan Fine Biotech Co., Ltd. (Wuhan, China). Briefly, a 96-well plate was pre-coated with monoclonal antibodies specific for Ki67, SOD1, CAT, and GPx. Standard references and the collected cell extracts were added to the wells and incubated for 90 min at 37 °C. Then, after the supernatant was removed, 100 μL biotinylated detection antibody was added for 60 min. After washing three times to remove any unbound substances, horseradish peroxidase-conjugated avidin was added to the wells. Following additional washing, 90 μL substrate solution was added to the wells for 15 min. Then, 50 μL reaction termination solution was added, and absorbance was measured at 450 nm using a microplate reader (FilterMax F5); this value was proportional to the amount of Ki67, SOD1, CAT, and GPx. The protein concentration was measured in each sample and determined in triplicate for each sample by using the Thermo Fisher NanoDrop device.

Enzyme Activity Assays

In all activity assays, the protein concentration was spectrophotometrically determined in triplicate for each sample at 280 nm by using the ND/1000 UV/Vis, Thermo Fisher NanoDrop device.

GPx Activity Assay

The activity of the GPx enzyme was assessed according to the manufacturer's protocol. All samples were prepared in either non-enzyme or enzyme tubes. The enzymatic reaction was prepared according to the schema: 0.2 mL of 1 mM GSH and 0.1 mL of reagent 1 were added to the enzyme tube. After incubation for 5 min in a water bath at 37 °C, 2 mL of reagent 2 was added. In the non-enzymatic tube, the sample was added after the addition of reagent 2. Following the addition of all components, the tubes were centrifuged at 3100×g for 10 min. After centrifugation, we added 1, 0.25, and 0.05 mL of reagents 3, 4, and 5, respectively, to 1 mL of supernatant. All the reagents were mixed and incubated for 15 min at room temperature. The OD values for each tube were measured at 412 nm using a microplate reader (ELISA LEDETECT 96).

SOD Activity Assay

The SOD activity was assessed according to the manufacturer's protocol. To the control well, we added 20 μL distilled water and 20 μL enzyme working solution. To

the control-blank well, we added 20 μL distilled water and 20 μL enzyme diluent. To the sample well, we added 20 μL sample and 20 μL enzyme working solution. To the sample-blank well, we added 20 μL sample and 20 μL enzyme diluent. Thereafter, 200 μL substrate solution was added to each well and the 96-well microplate was incubated at 37 °C for 20 min. The OD values were read at 450 nm using a microplate reader (ELISA LEDETECT 96).

CAT Activity Assay

The activity of the CAT enzyme was assessed according to the manufacturer's protocol. To the sample tube, we added 10 μL sample, 100 μL reagent 1, and 10 μL reagent 2, whereas we added only reagents 1 and 2 in the control tube. The tubes were shaken and incubated at 37 °C for 1 min. After incubation, reagent 3 (100 μL) and reagent 4 (10 μL) were added to the sample and control tubes, respectively; moreover, 10 μL sample was added to the control tube. The reagents were mixed and allowed to stand for 10 min at room temperature. The OD value of each tube (230 μL) was measured in a 96-well microplate at 405 nm using a microplate reader (ELISA LEDETECT 96).

Statistical Analysis

Data are presented as the mean ± standard deviation (SD) of three independent experiments. In each experiment, the treatment was repeated six times ($n = 6$). Data are presented as a percentage of the control and analyzed via one-way analysis of variance (ANOVA) followed by Tukey's multiple comparison procedure (p denotes the probability value; $***p < 0.001$, $**p < 0.01$, and $*p < 0.05$).

Results

ROS Production

After the SH-SY5Y cells were exposed to concentration of 100 pM to 100 μM VGVAPG for 3 h only in the range 50 nM to 50 μM, respectively, samples with the VGVAPG concentration showed increased ROS production by 33.98 to 37.82% compared to the control (Fig. 1a). Similarly, ROS production increased by 44.45 to 47.25% compared to the control (Fig. 1b) after SH-SY5Y cells were exposed for 6 h to concentrations of 10 nM to 50 μM VGVAPG.

On 24-h exposure of SH-SY5Y cells to 1 μM VGVAPG and 1 μM VVGPGA, respectively, only VGVAPG was shown to increase ROS production by 20.22% as compared to the
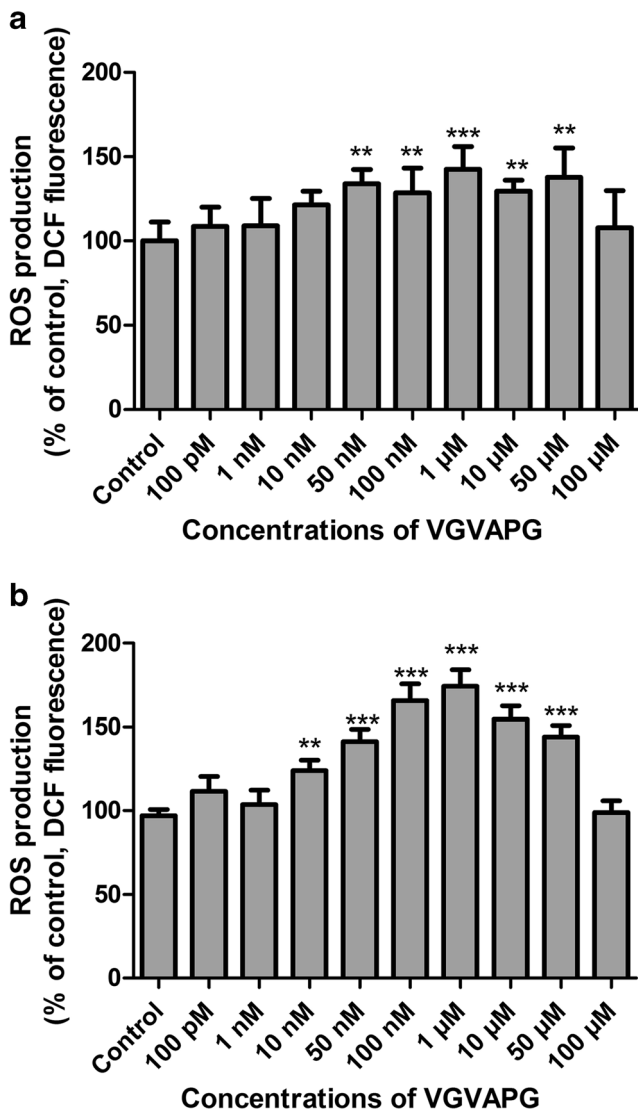
Fig. 1 Effect of different (100 pM to 100 μM) VGVAPG peptide concentrations on DCF fluorescence in the SH-SY5Y cell line. After **a** 3 h of exposure and **b** 6 h of exposure. Each point represents the mean ± SD of three independent experiments, each of which consisted of six replicates per treatment group. $**p < 0.01$, $***p < 0.001$, versus the control cells
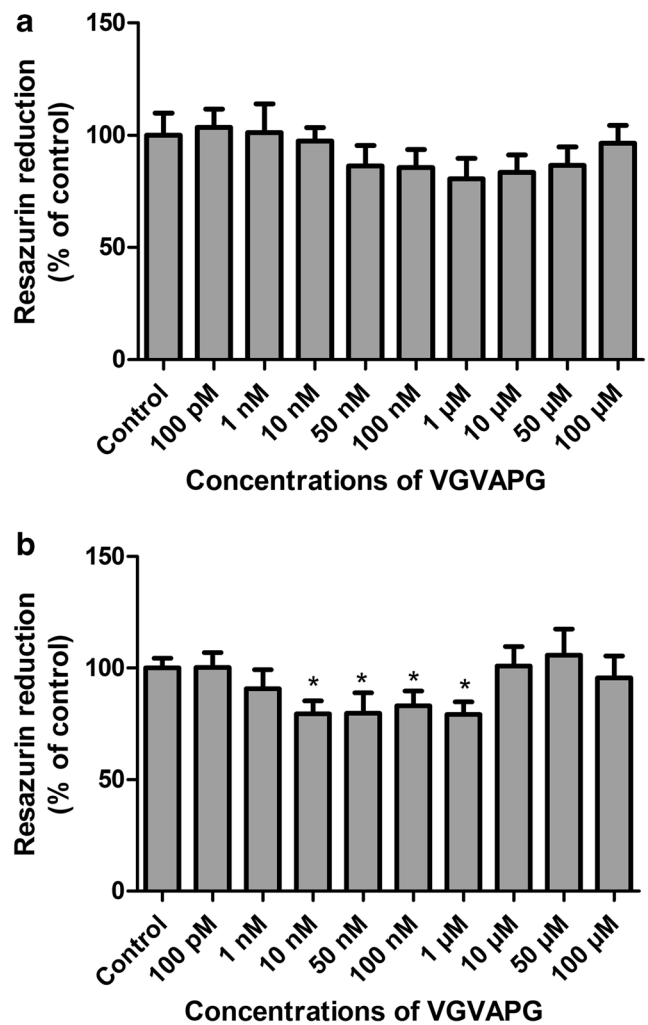

Fig. 2 The effect of different (100 pM to 100 μM) VGVAPG peptide concentrations on resazurin reduction in the SH-SY5Y cell line. After **a** 24 h of exposure and **b** 48 h of exposure. Each point represents the mean ± SD of three independent experiments, each of which consisted of six replicates per treatment group. $*p < 0.05$, versus the control cells

control. The NAC as a ROS scavenger did not affect ROS production as compared to the control; however, NAC as co-treatment with VGVAPG prevented ROS production (ROS production remained unchanged as compared to the control; Fig. 3a).

Resazurin Reduction Assay

No statistically significant decrease in resazurin reduction was observed as compared to the control after 24-h exposure of SH-SY5Y cells to concentrations of 100 pM to 100 μM VGVAPG; nevertheless, a downward trend was visible (Fig. 2a). Following 48-h exposure of SH-SY5Y cells to concentrations of 100 pM to 100 μM VGVAPG, we observed that

10 nM to 1 μM concentrations decreased resazurin reduction by 20.51 to 20.76% as compared to control (Fig. 2b).

After 24-h exposure of SH-SY5Y cells to 1 μM VGVAPG and 1 μM VVGPGA, we saw that only VGVAPG decreased resazurin reduction by 11.05% as compared to the control. Treatment with NAC alone caused an increase in resazurin reduction by 35.64% as compared to the control. However, NAC co-treatment with VGVAPG did not affect resazurin reduction when compared to the control (Fig. 3b).

Real-Time PCR Analysis of mRNAs

After 6-h exposure of SH-SY5Y cells to 50 nM and 1 μM VGVAPG peptide, the expression of *KI67* mRNA decreased by 27.77% and 31.50%, respectively, as compared to the control. However, the expression of *PPARγ* mRNA was unaffected by the VGVAPG peptide (Fig. 4a).
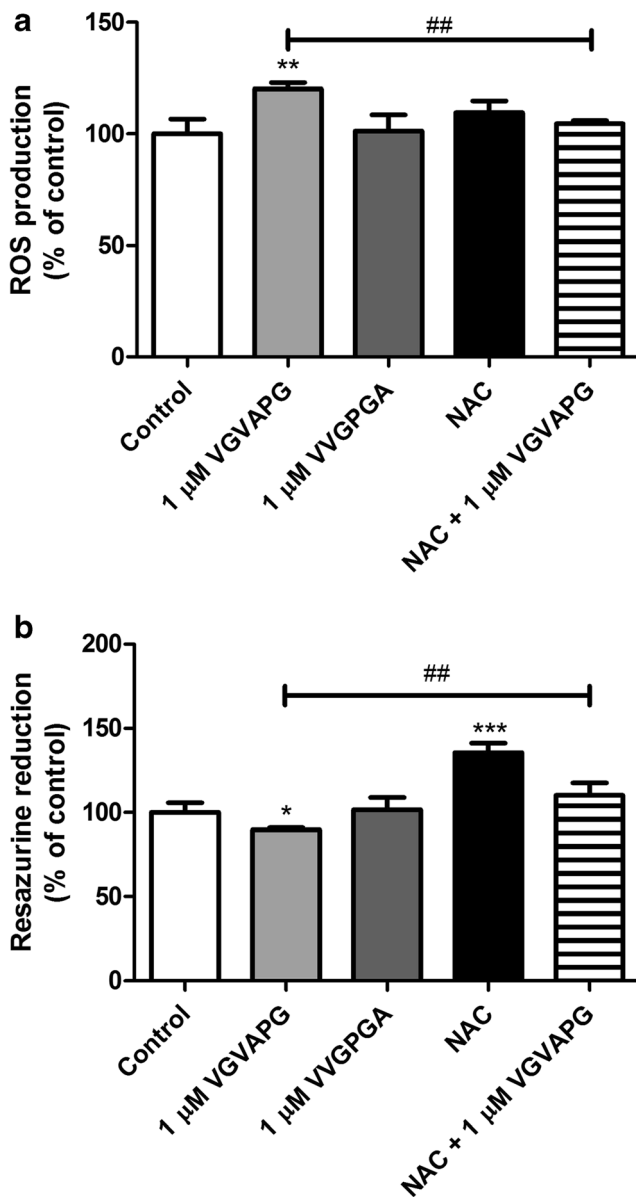
Fig. 3 a The effect of 1 μM VGVAPG peptide on ROS production in the SH-SY5Y cell line after 24 h. b The effect of 1 μM VGVAPG peptide on resazurin reduction in the SH-SY5Y cell line after 48 h. White bars represent control cells, gray bars show cells treated with 1 μM VGVAPG, black bars represent cells treated with NAC, and bars with stripes indicate cells co-treated with 1 μM VGVAPG and 1 μM NAC. Every point represents the mean ± SD of three independent experiments, each of which comprises six replicates per treatment group. *$p < 0.05$, **$p < 0.01$, ***$p < 0.001$, versus the control cultures. ##$p < 0.01$, VGVAPG versus VGVAPG with NAC

Enzyme-Linked Immunosorbent Assays

Ki67 Protein Expression

Exposure of SH-SY5Y cells to 50 nM and 1 μM VGVAPG peptide for 24 h did not change the expression of Ki67 protein; however, after 48-h exposure of
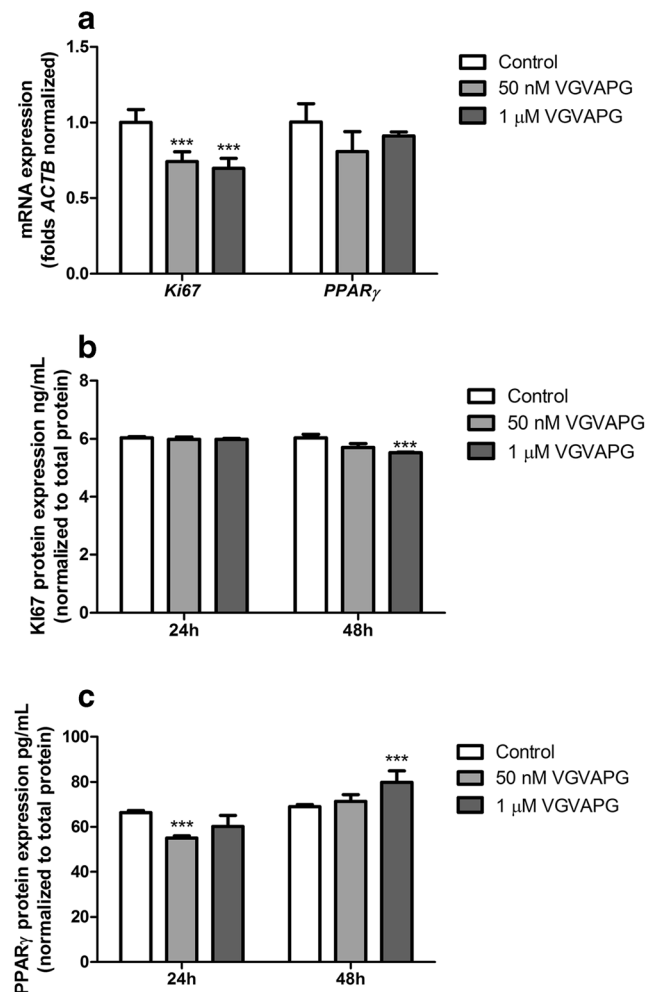

Fig. 4 a The effect of 50 nM and 1 μM VGVAPG peptide on Ki67 and PPARγ mRNA expression in the SH-SY5Y cell line after 6 h. mRNA expression was normalized to Actb. The effect of 50 nM and 1 μM VGVAPG peptide on b Ki67 and c PPARγ protein expression in the SH-SY5Y cell line after 24 and 48 h. Protein expression was normalized to the total protein level. Data are expressed as mean ± SD of three independent experiments, each of which comprised six replicates per treatment group. *$p < 0.05$; ***$p < 0.001$ versus the vehicle control

SH-SY5Y cells to 1 μM VGVAPG peptide, the expression of the Ki67 protein decreased by 0.51 ng/mL, compared to the control (Fig. 4b).

PPARγ Protein Expression

After 24-h exposure of SH-SY5Y cells to 50 nM VGVAPG peptide, the expression of PPARγ protein decreased by 11.33 pg/mL as compared to that with the control. Moreover, 48-h exposure of SH-SY5Y cells to 1 μM VGVAPG peptide increased the expression of PPARγ protein by 10.80 pg/mL as compared to the control (Fig. 4c).

GPx Protein Expression

After 24-h exposure of SH-SY5Y cells to VGVAPG peptide, the protein expression of GPx in the 1 μM concentration sample increased by 25.90 ng/mL. After 48-h of cell exposure to the VGVAPG peptide, the GPx protein expression increased in both concentrations—50 nM and 1 μM (increase of 60.34 and 54.28 ng/mL, respectively, compared to control; Fig. 5a).

SOD1 Protein Expression

Following 24-h exposure to VGVAPG peptide, the protein expression of SOD1 decreased for both the studied peptide concentrations (decreased by 8.15 and 8.29 pg/mL, respectively);

however, after 48-h exposure, the protein expression of SOD1 had not changed as compared to the control (Fig. 5b).

CAT Protein Expression

Exposure to VGVAPG peptide for 24 h resulted in a decrease of CAT protein expression by 18.95 ng/mL in the sample with a concentration of 1 μM as compared to the control; however, after 48-h exposure, CAT protein expression decreased for both the studied concentrations of 50 nM and 1 μM (decreased by 40.42 and 104.75 ng/mL respectively, compared to control; Fig. 5c).

Enzyme Activity Assays

GPx Activity Assay

Following 48-h exposure to 50 nM and 1 μM of VGVAPG peptide, GPx activity increased by 0.48 and 2.03 units, respectively, as compared to the control. The VVGPGA peptide does not affect GPx activity in SH-SY5Y cells. Silencing of the *GLB1* gene resulted in an increase in GPx activity by 1.15 units as compared to scramble-siRNA-treated cells; however, exposure of cells to 50 nM or 1 μM VGVAPG peptide decreased GPx activity to that of the *GLB1* siRNA control level. Silencing of the *LGALS3* gene induced an increase in GPx activity by 1.51 units as compared to that in scramble-siRNA-treated cells, whereas 50 nM and 1 μM VGVAPG reduced GPx activity by 0.50 and 1.00 units compared to the *LGALS3* siRNA control (Fig. 6a).

SOD Activity Assay

After 48-h exposure to 50 nM and 1 μM VGVAPG and 50 nM and 1 μM VVGPGA, none of the studied concentrations were found to affect SOD activity in SH-SY5Y cells. Silencing of the *GLB1* gene induced an increase in SOD activity by 0.81 units compared to scramble-siRNA-treated cells; however, exposure of cells to 50 nM or 1 μM VGVAPG peptide decreased SOD activity to the *GLB1* siRNA control level. Silencing of the *LGALS3* gene does not affect SOD activity in SH-SY5Y cells (Fig. 6b).

CAT Activity Assay

After 48-h exposure to 50 nM and 1 μM of VGVAPG and 50 nM and 1 μM VVGPGA, none of the studied concentrations were found to affect CAT activity in SH-SY5Y cells. Silencing of the *GLB1* gene does not affect CAT activity in SH-SY5Y cells; however, exposure of cells to 1 μM VGVAPG peptide induced an increase in CAT activity by 0.73 units compared to the *GLB1* siRNA control level. Silencing of the *LGALS3* gene resulted in a decrease in CAT
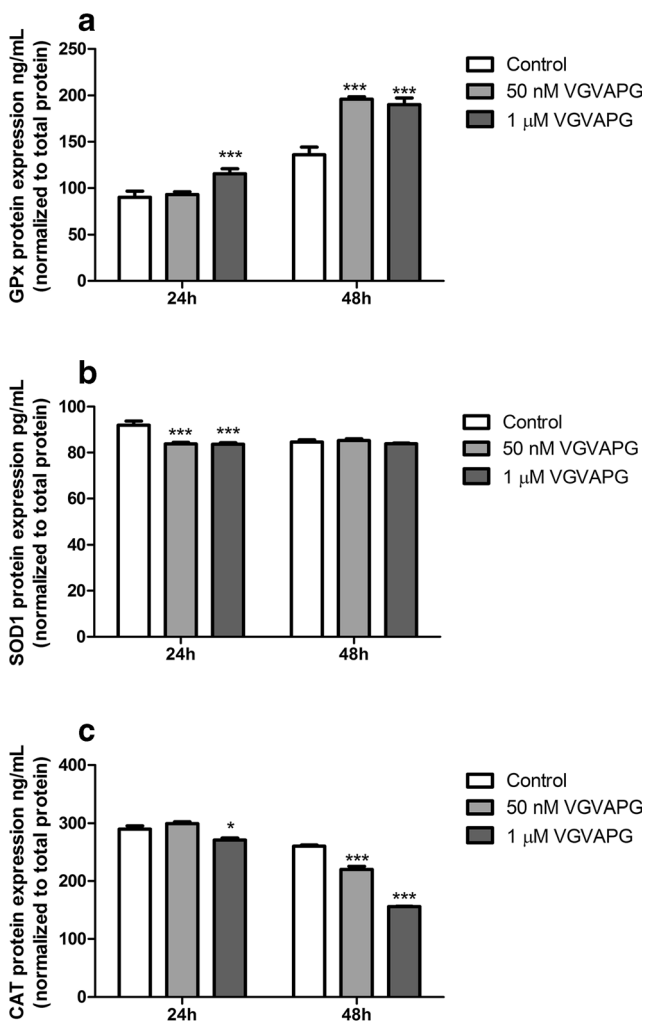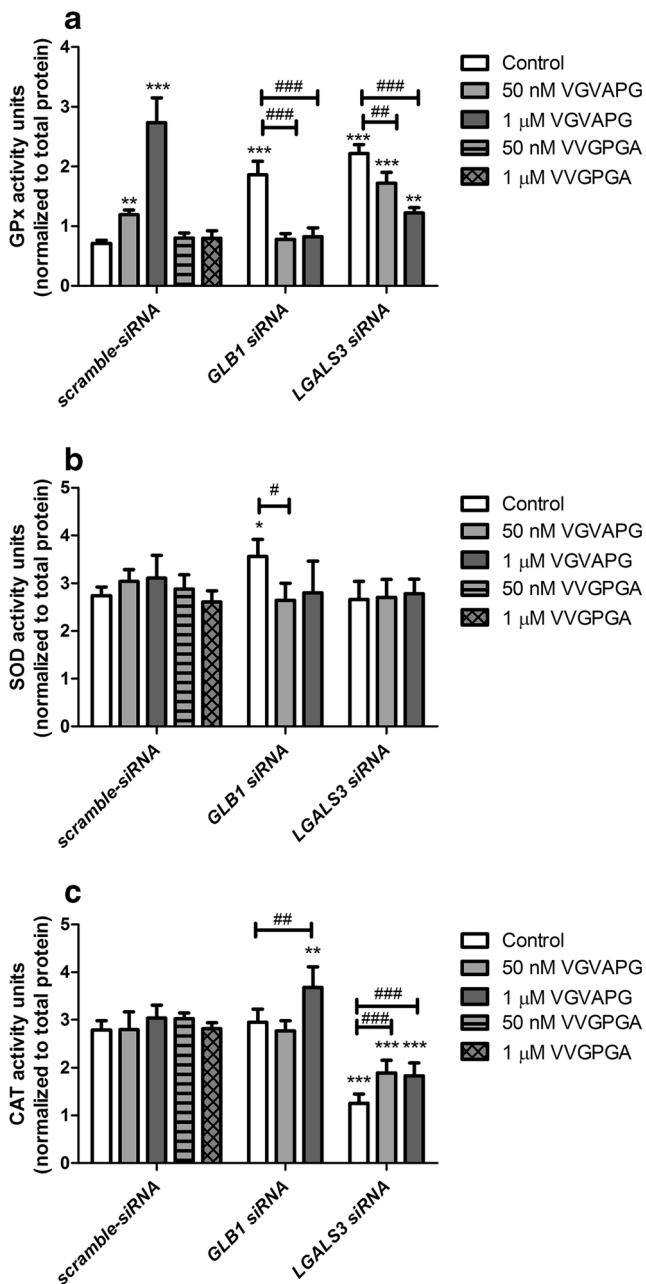

Fig. 5 The effect of 50 nM and 1 μM VGVAPG peptide on **a** GPx, **b** SOD1, and **c** CAT protein expression in the SH-SY5Y cell line after 24 and 48 h of exposure. Protein expression was normalized to the total protein level. Data are expressed as mean ± SD of three independent experiments, each of which consisted of six replicates per treatment group. *$p < 0.05$; ***$p < 0.001$ versus the vehicle control

Fig. 6 The effect of 50 nM and 1 μM of VGVAPG and VVGPGA peptide, respectively, on **a** GPx, **b** SOD, and **c** CAT activity in the SH-SY5Y cell line after 48 h. The experiments were conducted after application of scrambled siRNA, *GLB1* siRNA, or *LGAL3* siRNA. Protein activity was normalized to the total protein level. Data are expressed as mean ± SD of three independent experiments, each of which consisted of six replicates per treatment group. *$p < 0.05$; ***$p < 0.001$ versus the scramble siRNA vehicle control. #$p < 0.05$; ##$p < 0.01$; ###$p < 0.001$ versus the *GLB1* siRNA, or *LGAL3* siRNA vehicle control

activity by 1.53 units as compared to the scramble-siRNA-treated cells. After *LGALS3* gene silencing, exposure of cells to 50 nM and 1 μM VGVAPG induced an increase in CAT activity by 0.64 and 0.58 units, respectively, compared to the *LGALS3* siRNA control (Fig. 6c).

Discussion

This study presents the first data from an investigation of the impact of VGVAPG peptides on SH-SY5Y cells. The experiments revealed that, after 3 and 6 h, VGVAPG peptides at a wide range of concentrations (10 nM to 50 μM) increase ROS production in SH-SY5Y cells, whereas a random peptide sequence (VVGPGA) does not affect ROS production. To date, similar results were obtained by our research group in mouse primary astrocytes. In mouse primary cells, the VGVAPG peptide induced an increase in ROS production in all studied concentrations (100 pM to 100 μM) (Szychowski and Gmiński 2019a). Moreover, it had been described that the κ-elastin and VGVAPG peptide increases ROS production in murine monocytes and human fibroblasts (Robert et al. 1984; Gayral et al. 2014; Scandolera et al. 2015). Scandolera et al. (2015) described that, in an in vitro model of aging, the ROS level in fibroblasts increased, whereas the proliferation potential decreased (Scandolera et al. 2015). Furthermore, during in vitro aging, the proliferatory potential of the VGVAPG peptide was reduced. Due to the key role of ROS in cell signaling, cell death, and aging, we decide to measure the metabolism and proliferation potential of SH-SY5Y cells.

Our data show that, after 24 and 48 h of stimulation of SH-SY5Y cells by the VGVAPG peptide, cell metabolism/proliferation decreased, as measured by the resazurin assay. This decrease in cell metabolism/proliferation was observed in similar concentrations that also caused an increase in ROS production, whereas a random peptide sequence (VVGPGA) did not affect cell metabolism/proliferation. The decrease in the proliferation rate was confirmed by mRNA and protein expression of Ki67 protein, which is an established marker of cell proliferation. To date, it is believed that activation of EBP increases the proliferation of human lymphocytes, fibroblasts, melanoma, astrocytoma, glioma, and endothelial cells (Péterszegi et al. 1996; Tajima et al. 1997; Jung et al. 1998; Hinek et al. 1999; Dutoya et al. 2000; Devy et al. 2010). However, some authors described that, based on the concentration, κ-elastin can stimulate not only proliferation but also cell death (Péterszegi and Robert 1998). Péterszegi and Robert showed that lymphocytes exposed to 1–10 μg/mL of κ-elastin do proliferate; however, when the concentration was greater than 100 μg/mL, cell death was apparent. Interestingly, cells died through both apoptotic and non-apoptotic mechanisms (Péterszegi and Robert 1998). However, in our previous studies, we did not observe an increase in lactate dehydrogenase (LDH) release, which is a marker of necrosis or secondary necrosis (after the disintegration of apoptotic bodies in an in vitro model) in mouse astrocytes stimulated by the VGVAPG peptide (Szychowski et al. 2019b). On the other hand, EDP and/or VGVAPG induce an increase in cell chemotaxis and migration (mainly in cancerous cells) that can lead to decreased cell proliferation without a reduction in cell

viability as a result of cell movement (Scandolera et al. 2016). Our previous studies show that the VGVAPG peptide activates and increases PPARγ mRNA and protein expression in mouse astrocytes in vitro (Szychowski and Gmiński 2019b). To date, it is well described that PPARγ stops cell proliferation and promotes cell differentiation (Wada et al. 2006; Stergiopoulos and Politis 2013).

To elucidate the involvement of ROS in decreased cell proliferation, the ROS scavenger NAC was employed. Our experiments show that NAC decreases ROS production that was stimulated by the VGVAPG peptide. Moreover, NAC itself increased SH-SY5Y proliferation when measured by the resazurin reduction assay, and this was confirmed by the ELISA measurement of Ki67 protein. In cells co-treated with NAC and VGVAPG, we did not observe any changes as compared to control cells. Our data suggest that, in SH-SY5Y cells, ROS is a key element to decrease cell proliferation.

To date, it has been well described that the VGVAPG peptide probably acts only through receptors on the cell surface (Senior et al. 1984; Blood et al. 1988; Maurice et al. 2013). Our previous study showed that, in mouse astrocytes, ROS production was dependent on EBP and, after *Glb1* silencing, the VGVAPG peptide did not activate ROS production in mouse astrocytes in vitro (Szychowski and Gmiński 2019a). Therefore, the next step of our study was to investigate the effect of silencing of *GLB1* and *LGALS3* genes in SH-SY5Y cells. Our data show that after stimulation of SH-SY5Y cells by the VGVAPG peptide, GPx activity increased, whereas silencing of the *GLB1* gene prevented this process. Silencing of the *LGALS3* gene partially prevents an increase in GPx activity induced by the VGVAPG peptide. Interestingly, the silencing process of *GLB1* and *LGALS3* itself induces an increase in GPx activity. We did not observe any changes in SOD activity. Similar to previous findings, the silencing of *GLB1* itself induced an increase in SOD activity in the control group. In contrast to protein expression, CAT activity did not change. The silencing of the *LGALS3* gene decreased CAT activity in the group treated with VGVAPG. The addition of a random peptide sequence (VVGPGA) did not affect the activity of any of the studied enzymes. The effects of the *GLB1* and *LGALS3* gene silencing itself on the activity of antioxidant enzymes are probably the result of a role of β-galactosidase and galectin-3 in cells. Based on our data, we believe that both EBP and galectin-3 receptors are involved in the regulation of activity of antioxidant enzymes in SH-SY5Y cells. Moreover, our experiments show that, after 48-h exposure, the VGVAPG peptide increased GPx expression, did not affect SOD1 expression, and decreased CAT protein expression in SH-SY5Y cells.

To date, data on the activity of antioxidant enzymes after treatment with EDPs or VGVAPG are very limited. Gmiński et al. showed that κ-elastin increases the activities of SOD, CAT, and GPx as well as lipid peroxidation in human

fibroblasts (Gmiński et al. 1991). On the other hand, the VGVAPG peptide reduced ROS production in neutrophils (Dupont et al. 2013). However, in our opinion, the results obtained by Dupont et al. (2013) were probably an effect of the increased expression of antioxidant enzymes. It is noteworthy that, in our experiments, the highest level of ROS was noted after 6-h exposure to VGVAPG. However, after 24-h cell treatment with 1 μM VGVAPG peptide, the level of ROS was lower than that recorded after 6-h exposure to the VGVAPG peptide. Our results are probably an effect of the increasing expression and/or activity of GPx. To date, it is well described that PPARγ activation decreases ROS production through the involvement of NF-κB and also increases the production of antioxidant enzymes (Lee et al. 2006; Jung et al. 2007). We previously described that the VGVAPG peptide activates the PPARγ receptor in mouse astrocytes in vitro (Szychowski and Gmiński 2019b). A similar phenomenon was observed in SH-SY5Y cells. After 24-h exposure to VGVAPG, the expression of PPARγ protein slightly decreased in SH-SY5Y cells, which is an effect of receptor degradation after activation. However, after 48-h exposure of SH-SY5Y cells to VGVAPG, the PPARγ protein expression increased. Despite the fact that we show that the VGVAPG peptide increased GPx activity, ROS production increased in SH-SY5Y cells at least for short intervals (up to 6 h). Due to the long duration needed to produce antioxidant enzymes, we believe that this phenomenon is the cause of the postponement of ROS reduction that was observed by other authors. Similar to our data, elevated ROS levels and activities of antioxidant enzyme were previously described in C57BL/6 mice and in the SH-SY5Y cell line models of Parkinson's disease (Cassarino et al. 1997). In our opinion, the primary reason for the rapid increase in ROS level could be excitotoxicity caused by VGVAPG in neuroblastoma cells. To date, it is well described that the N-methyl-D-aspartic acid receptor (NMDAR) is involved in excitotoxicity-induced cell death in human embryonic stem cell–derived neurons, neuroblasts, and neuroblastoma cells (Sun et al. 2010; Gupta et al. 2013; Nato et al. 2015). NMDAR-mediated excitotoxicity is Ca^{2+}-dependent and is typical in the nervous system (Dong et al. 2009). Numerous reports have shown that κ-elastin, EDPs, and the VGVAPG peptide activate the influx of Ca^{2+} into cells, and this process requires EBP activation (Jacob et al. 1987; Faury et al. 1998a, b; Maurice et al. 2013). Different authors have suggested that G proteins and c-Src as well as ERK1/2 or MEK1/2 kinases are involved in signal transduction; however, the molecular mechanism mediating the opening of Ca^{2+} channels remains unclear (Mochizuki et al. 2002; Fahem et al. 2008; Maurice et al. 2013). Moreover, it has been shown that EBP is internalized after activation; therefore, we cannot exclude that VGVAPG or EDP can act from within the cell on cell metabolism (Hinek et al. 1995). In our opinion, excitotoxicity mediated through NMDAR and dependent on

ROS production is the likely cause of the decrease in the level of the cell proliferation marker Ki67.

Conclusion

The VGVAPG peptide increases GPx expression and activity in the SH-SY5Y cell line. Silencing of the *GLB1* gene prevents changes in GPx activity. Despite the fact that the VGVAPG peptide increases GPx expression, it increases the ROS level. Moreover, the VGVAPG peptide induced a decrease in SH-SY5Y proliferation that was prevented by the ROS scavenger NAC. ROS production and decreased proliferation of SH-SY5Y cells are the results of excitotoxicity mediated through a close unrecognized molecular pathway. More studies are needed to elucidate the presently unknown mechanism of action of the VGVAPG peptide in the nervous system.

Compliance with Ethical Standards

Conflict of Interest The authors declare that they have no conflict of interest.

Abbreviations *CAT,* Catalase; *DMSO,* Dimethyl sulfoxide; *EBP,* Elastin-binding protein; *ECM,* Extracellular matrix; *EDPs,* Elastin-derived peptides; *FBS,* Fetal bovine serum; *gal-3,* Galectin-3; *GPx,* Glutathione peroxidase; *PBS,* Phosphate-buffered saline; *PPARγ,* Peroxisome proliferator-activated receptor gamma; *ROS,* Reactive oxygen species; *siRNA,* Small interfering RNA; *SOD,* Superoxide dismutase; *VGVAPG,* Val-Gly-Val-Ala-Pro-Gly; *β-Gal,* Beta-galactosidase

References

Apple DM, Solano-Fonseca R, Kokovay E (2017) Neurogenesis in the aging brain. Biochem Pharmacol 141:77–85. https://doi.org/10.1016/j.bcp.2017.06.116

Blood CH, Sasse J, Brodt P, Zetter BR (1988) Identification of a tumor cell receptor for VGVAPG, an elastin-derived chemotactic peptide. J Cell Biol 107:1987–1993. https://doi.org/10.1083/jcb.107.5.1987

Bresalier RS, Byrd JC, Wang L, Raz A (1996) Colon cancer mucin: a new ligand for the β-galactoside-binding protein galectin-3. Cancer Res 56:4354–4357

Cantarelli B, Duca L, Blanchevoye C, Poitevin S, Martiny L, Debelle L (2009) Elastin peptides antagonize ceramide-induced apoptosis. FEBS Lett 583:2385–2391. https://doi.org/10.1016/j.febslet.2009.06.037

Cassarino DS, Fall CP, Swerdlow RH, Smith TS, Halvorsen EM, Miller SW, Parks JP, Parker WD Jr, Bennett JP Jr (1997) Elevated reactive oxygen species and antioxidant enzyme activities in animal and cellular models of Parkinson's disease. Biochim Biophys Acta Mol Basis Dis 1362:77–86. https://doi.org/10.1016/S0925-4439(97)00070-7

Chiappini C, Berliocchi L, Cerri S et al (2018) Early LC3 lipidation induced by d-limonene does not rely on mTOR inhibition, ERK activation and ROS production and it is associated with reduced clonogenic capacity of SH-SY5Y neuroblastoma cells. Phytomedicine 40:98–105. https://doi.org/10.1016/j.phymed.2018.01.005

Coquerel B, Poyer F, Torossian F, Dulong V, Bellon G, Dubus I, Reber A, Vannier JP (2009) Elastin-derived peptides: Matrikines critical for glioblastoma cell aggressiveness in a 3-D system. Glia 57:1716–1726. https://doi.org/10.1002/glia.20884

Desforges M, Harris LK, Aplin JD (2014) Elastin-derived peptides stimulate trophoblast migration and invasion: a positive feedback loop to enhance spiral artery remodelling. Mol Hum Reprod 21:95–104. https://doi.org/10.1093/molehr/gau089

Devy J, Duca L, Cantarelli B, Joseph-Pietras D, Scandolera A, Rusciani A, Parent L, Thevenard J, Pasco SB, Tarpin M, Martiny L, Debelle L (2010) Elastin-derived peptides enhance melanoma growth in vivo by upregulating the activation of Mcol-A (MMP-1) collagenase. Br J Cancer 103:1562–1570. https://doi.org/10.1038/sj.bjc.6605926

Dong X, Wang Y, Qin Z (2009) Molecular mechanisms of excitotoxicity and their relevance to pathogenesis of neurodegenerative diseases. Acta Pharmacol Sin 30:379–387. https://doi.org/10.1038/aps.2009.24

Dupont A, Dury S, Gafa V, Lebargy F, Deslée G, Guenounou M, Antonicelli F, le Naour R (2013) Impairment of neutrophil reactivity to elastin peptides in COPD. Thorax 68:421–428. https://doi.org/10.1136/thoraxjnl-2012-201833

Dutoya S, Lefeèbvre F, Rabaud M, Verna A (2000) Elastin-derived protein coating onto poly(ethylene terephthalate). Technical, microstructural and biological studies. Biomaterials 21:1521–1529. https://doi.org/10.1016/S0142-9612(99)00274-4

Fahem A, Robinet A, Cauchard JH, Duca L, Soula-Rothhut M, Rothhut B, Soria C, Guenounou M, Hornebeck W, Bellon G (2008) Elastokine-mediated up-regulation of MT1-MMP is triggered by nitric oxide in endothelial cells. Int J Biochem Cell Biol 40:1581–1596. https://doi.org/10.1016/j.biocel.2007.11.022

Faury G, Garnier S, Weiss AS et al (1998a) Action of tropoelastin and synthetic elastin sequences on vascular tone and on free Ca2+ level in human vascular endothelial cells. Circ Res 82:328–336

Faury G, Usson Y, Robert-Nicoud M, Robert L, Verdetti J (1998b) Nuclear and cytoplasmic free calcium level changes induced by elastin peptides in human endothelial cells. Proc Natl Acad Sci U S A 95:2967–2972. https://doi.org/10.1073/pnas.95.6.2967

Gayral S, Garnotel R, Castaing-Berthou A, Blaise S, Fougerat A, Berge E, Montheil A, Malet N, Wymann MP, Maurice P, Debelle L, Martiny L, Martinez LO, Pshezhetsky AV, Duca L, Laffargue M (2014) Elastin-derived peptides potentiate atherosclerosis through the immune Neu1-PI3K pathway. Cardiovasc Res 102:118–127. https://doi.org/10.1093/cvr/cvt336

Glennon-Alty L, Hackett AP, Chapman EA, Wright HL (2018) Neutrophils and redox stress in the pathogenesis of autoimmune disease. Free Radic Biol Med 125:25–35. https://doi.org/10.1016/j.freeradbiomed.2018.03.049

Gmiński J, W glarz L, Dróżdż M, Goss M (1991) Pharmacological modulation of the antioxidant enzymes activities and the concentration of peroxidation products in fibroblasts stimulated with elastin

peptides. Gen Pharmacol Vasc Syst 22:495–497. https://doi.org/10.1016/0306-3623(91)90012-U

Gminski J, Mykala-Ciesla J, Machalski M, Drozdz M (1993) Elastin metabolism parameters in sera of patients with lung cancer. Neoplasma 40:41–44

Gupta K, Hardingham GE, Chandran S (2013) NMDA receptor-dependent glutamate excitotoxicity in human embryonic stem cell-derived neurons. Neurosci Lett 543:95–100. https://doi.org/10.1016/j.neulet.2013.03.010

Hämmerle B, Yañez Y, Palanca S, Cañete A, Burks DJ, Castel V, Font de Mora J (2013) Targeting neuroblastoma stem cells with retinoic acid and proteasome inhibitor. PLoS One 8:1–15. https://doi.org/10.1371/journal.pone.0076761

Hinek A, Rabinovitch M, Keeley F, Okamura-Oho Y, Callahan J (1993) The 67-kD elastin/laminin-binding protein is related to an enzymatically inactive, alternatively spliced form of beta-galactosidase. J Clin Invest 91:1198–1205. https://doi.org/10.1172/JCI116280

Hinek A, Keeley FW, Callahans J (1995) Recycling of the 67-kDa elastin binding protein in arterial myocytes is imperative for secretion of tropoelastin. Exp Cell Res 220:312–324. https://doi.org/10.1006/excr.1995.1321

Hinek A, Jung S, Rutka JT (1999) Cell surface aggregation of elastin receptor molecules caused by suramin amplified signals leading to proliferation of human glioma cells. Acta Neuropathol 97:399–407

Inohara H, Akahani S, Raz A (1998) Galectin-3 stimulates cell proliferation. Exp Cell Res 245:294–302. https://doi.org/10.1006/excr.1998.4253

Jacob MP, Fülöp T, Foris G, Robert L (1987) Effect of elastin peptides on ion fluxes in mononuclear cells, fibroblasts, and smooth muscle cells. Proc Natl Acad Sci U S A 84:995–999. https://doi.org/10.1073/pnas.84.4.995

Jung S, Rutka JT, Hinek A (1998) Tropoelastin and elastin degradation products promote proliferation of human astrocytoma cell lines. J Neuropathol Exp Neurol 57:439–448. https://doi.org/10.1097/00005072-199805000-00007

Jung TW, Lee JY, Shim WS, Kang ES, Kim SK, Ahn CW, Lee HC, Cha BS (2007) Rosiglitazone protects human neuroblastoma SH-SY5Y cells against MPP+ induced cytotoxicity via inhibition of mitochondrial dysfunction and ROS production. J Neurol Sci 253:53–60. https://doi.org/10.1016/j.jns.2006.11.020

Kamoun A, Landeau JM, Godeau G, Wallach J, Duchesnay A, Pellat B, Hornebeck W (1995) Growth stimulation of human skin fibroblasts by elastin-derived peptides. Cell Adhes Commun 3:273–281

Kim GH, Kim JE, Rhie SJ, Yoon S (2015) The role of oxidative stress in neurodegenerative diseases. Exp Neurobiol 24:325. https://doi.org/10.5607/en.2015.24.4.325

Kołodziej U, Maciejczyk M, Zalewska A (2018) Oxidative stress – repair systems of oxidatively damaged biomolecules. Prog Heal Sci 8:141–150. https://doi.org/10.5604/01.3001.0012.1118

Lee KS, Kim SR, Park SJ, Park HS, Min KH, Jin SM, Lee MK, Kim UH, Lee YC (2006) Peroxisome proliferator activated receptor-γ modulates reactive oxygen species generation and activation of nuclear factor-κB and hypoxia-inducible factor 1α in allergic airway disease of mice. J Allergy Clin Immunol 118:120–127. https://doi.org/10.1016/j.jaci.2006.03.021

Maurice P, Blaise S, Gayral S, Debelle L, Laffargue M, Hornebeck W, Duca L (2013) Elastin fragmentation and atherosclerosis progression: the elastokine concept. Trends Cardiovasc Med 23:211–221. https://doi.org/10.1016/j.tcm.2012.12.004

Mochizuki S, Brassart B, Hinek A (2002) Signaling pathways transduced through the elastin receptor facilitate proliferation of arterial smooth muscle cells. J Biol Chem 277:44854–44863. https://doi.org/10.1074/jbc.M205630200

Nato G, Caramello A, Trova S, Avataneo V, Rolando C, Taylor V, Buffo A, Peretto P, Luzzati F (2015) Striatal astrocytes produce neuroblasts

in an excitotoxic model of Huntington's disease. Development 142:840–845. https://doi.org/10.1242/dev.116657

Nita M, Grzybowski A (2016) The role of the reactive oxygen species and oxidative stress in the pathomechanism of the age-related ocular diseases and other pathologies of the anterior and posterior eye segments in adults. Oxidative Med Cell Longev 2016:1–23. https://doi.org/10.1155/2016/3164734

Ochieng J, Warfield P, Green-Jarvis B, Fentie I (1999) Galectin-3 regulates the adhesive interaction between breast carcinoma cells and elastin. J Cell Biochem 75:505–514

Ochieng J, Furtak V, Lukyanov P (2002) Extracellular functions of galectin-3. Glycoconj J 19:527–535. https://doi.org/10.1023/B:GLYC.0000014082.99675.2f

Oh J, Lee YD, Wagers AJ (2014) Stem cell aging: mechanisms, regulators and therapeutic opportunities. Nat Med 20:870–880. https://doi.org/10.1038/nm.3651

Péterszegi G, Robert L (1998) Cell death induced in lymphocytes expressing the elastin-laminin receptor by excess agonists: necrosis and apoptosis. Biomed Pharmacother 52:369–377. https://doi.org/10.1016/S0753-3322(99)80004-3

Péterszegi G, Robert AM, Robert L (1996) Presence of the elastin-laminin receptor on human activated lymphocytes. C R Acad Sci III 319:799–803

Pocza P, Süli-Vargha H, Darvas Z, Falus A (2008) Locally generated VGVAPG and VAPG elastin-derived peptides amplify melanoma invasion via the galectin-3 receptor. Int J Cancer 122:1972–1980. https://doi.org/10.1002/ijc.23296

Robert L, Jacob MP, Frances C, Godeau G, Hornebeck W (1984) Interaction between elastin and elastases and its role in the aging of the arterial wall, skin and other connective tissues. A review. Mech Ageing Dev 28:155–166

Ross RA, Walton JD, Han D, Guo HF, Cheung NKV (2015) A distinct gene expression signature characterizes human neuroblastoma cancer stem cells. Stem Cell Res 15:419–426. https://doi.org/10.1016/j.scr.2015.08.008

Sasaki T, Awaji T, Shimada K, Sasaki H (2018) Increased levels of reactive oxygen species in brain slices after transient hypoxia induced by a reduced oxygen supply. Neuropsychiatry 8:684–690. https://doi.org/10.4172/Neuropsychiatry.1000392

Scandolera A, Rabenoelina F, Chaintreuil C, Rusciani A, Maurice P, Blaise S, Romier-Crouzet B, el Btaouri H, Martiny L, Debelle L, Duca L (2015) Uncoupling of elastin complex receptor during in vitro aging is related to modifications in its intrinsic sialidase activity and the subsequent lactosylceramide production. PLoS One 10:e0129994. https://doi.org/10.1371/journal.pone.0129994

Scandolera A, Odoul L, Salesse S, Guillot A, Blaise S, Kawecki C, Maurice P, el Btaouri H, Romier-Crouzet B, Martiny L, Debelle L, Duca L (2016) The elastin receptor complex: a unique matricellular receptor with high anti-tumoral potential. Front Pharmacol 7:1–10. https://doi.org/10.3389/fphar.2016.00032

Senior RM, Griffin GL, Mecham RP et al (1984) Val-Gly-Val-Ala-Pro-Gly, a repeating peptide in elastin, is chemotactic for fibroblasts and monocytes. J Cell Biol 99:870–874. https://doi.org/10.1083/jcb.99.3.870

Skeie JM, Hernandez J, Hinek A, Mullins RF (2012) Molecular responses of choroidal endothelial cells to elastin derived peptides through the elastin-binding protein (GLB1). Matrix Biol 31:113–119. https://doi.org/10.1016/j.matbio.2011.11.003

Stergiopoulos A, Politis PK (2013) The role of nuclear receptors in controlling the fine balance between proliferation and differentiation of neural stem cells. Arch Biochem Biophys 534:27–37. https://doi.org/10.1016/j.abb.2012.09.009

Sun Z-W, Zhang L, Zhu S-J, Chen WC, Mei B (2010) Excitotoxicity effects of glutamate on human neuroblastoma SH-SY5Y cells via oxidative damage. Neurosci Bull 26:8–16. https://doi.org/10.1007/s12264-010-0813-7

Szychowski KA, Gmiński J (2019a) The VGVAPG peptide regulates the production of nitric oxide synthases and reactive oxygen species in mouse astrocyte cells in vitro. Neurochem Res. 44:1127-1137. https://doi.org/10.1007/s11064-019-02746-z

Szychowski KA, Gmiński J (2019b) Impact of elastin-derived VGVAPG peptide on bidirectional interaction between peroxisome proliferator-activated receptor gamma (Pparγ) and beta-galactosidase (β-Gal) expression in mouse cortical astrocytes in vitro. Naunyn Schmiedeberg's Arch Pharmacol 392:405–413. https://doi.org/10.1007/s00210-018-1591-4

Szychowski KA, Wójtowicz AK (2016) TBBPA causes neurotoxic and the apoptotic responses in cultured mouse hippocampal neurons in vitro. Pharmacol Reports 68:20–26. https://doi.org/10.1016/j.pharep.2015.06.005

Szychowski KA, Leja ML, Kaminskyy DV, Binduga UE, Pinyazhko OR, Lesyk RB, Gmiński J (2017a) Study of novel anticancer 4-thiazolidinone derivatives. Chem Biol Interact 262:46–56. https://doi.org/10.1016/j.cbi.2016.12.008

Szychowski KA, Leja ML, Kaminskyy DV, Kryshchyshyn AP, Binduga UE, Pinyazhko OR, Lesyk RB, Tobiasz J, Gmiński J (2017b) Anticancer properties of 4-thiazolidinone derivatives depend on peroxisome proliferator-activated receptor gamma (PPARγ). Eur J Med Chem 141:162–168. https://doi.org/10.1016/j.ejmech.2017.09.071

Szychowski KA, Wnuk A, Rzemieniec J, Kajta M, Leszczyńska T, Wójtowicz AK (2019a) Triclosan-evoked neurotoxicity involves NMDAR subunits with the specific role of GluN2A in caspase-3-dependent apoptosis. Mol Neurobiol 56:1–12. https://doi.org/10.1007/s12035-018-1083-z

Szychowski KA, Wójtowicz AK, Gmiński J (2019b) Impact of elastin-derived peptide VGVAPG on matrix metalloprotease-2 and -9 and the tissue inhibitor of metalloproteinase-1, -2, -3 and -4 mRNA expression in mouse cortical glial cells in vitro. Neurotox Res 35:100–110. https://doi.org/10.1007/s12640-018-9935-x

Tajima S, Wachi H, Uemura Y, Okamoto K (1997) Modulation by elastin peptide VGVAPG of cell proliferation and elastin expression in human skin fibroblasts. Arch Dermatol Res 289:489–492. https://doi.org/10.1007/s004030050227

Toupance S, Brassart B, Rabenoelina F, Ghoneim C, Vallar L, Polette M, Debelle L, Birembaut P (2012) Elastin-derived peptides increase invasive capacities of lung cancer cells by post-transcriptional regulation of MMP-2 and uPA. Clin Exp Metastasis 29:511–522. https://doi.org/10.1007/s10585-012-9467-3

Uğuz AC, Öz A, Nazıroğlu M (2016) Curcumin inhibits apoptosis by regulating intracellular calcium release, reactive oxygen species and mitochondrial depolarization levels in SH-SY5Y neuronal cells. J Recept Signal Transduct 36:395–401. https://doi.org/10.3109/10799893.2015.1108337

Venkatesh Gobi V, Rajasankar S, Ramkumar M, Dhanalakshmi C, Manivasagam T, Justin Thenmozhi A, Essa MM, Chidambaram R (2018) Agaricus blazei extract attenuates rotenone-induced apoptosis through its mitochondrial protective and antioxidant properties in SH-SY5Y neuroblastoma cells. Nutr Neurosci 21:97–107. https://doi.org/10.1080/1028415X.2016.1222332

Wada K, Nakajima A, Katayama K, Kudo C, Shibuya A, Kubota N, Terauchi Y, Tachibana M, Miyoshi H, Kamisaki Y, Mayumi T, Kadowaki T, Blumberg RS (2006) Peroxisome proliferator-activated receptor gamma-mediated regulation of neural stem cell proliferation and differentiation. J Biol Chem 281:12673–12681. https://doi.org/10.1074/jbc.M513786200

Walton JD, Kattan DR, Thomas SK, Spengler BA, Guo HF, Biedler JL, Cheung NKV, Ross RA (2004) Characteristics of stem cells from human neuroblastoma cell lines and in tumors. Neoplasia 6:838–845. https://doi.org/10.1593/neo.04310

Wang Y, Nangia-Makker P, Tait L, Balan V, Hogan V, Pienta KJ, Raz A (2009) Regulation of prostate cancer progression by galectin-3. Am J Pathol 174:1515–1523. https://doi.org/10.2353/ajpath.2009.080816